

UCLA

UCLA Previously Published Works

Title

Mt. Vettore Fault Zone Rupture: LIDAR- and UAS-Based Structure-From-Motion  
Computational Imaging

Permalink

<https://escholarship.org/uc/item/183128x1>

Authors

Kayen, Robert E

Gori, Stefano

Lingwall, Bret

et al.

Publication Date

2023-12-12

Peer reviewed

## MT. VETTORE FAULT ZONE RUPTURE: LIDAR- AND UAS-BASED STRUCTURE-FROM-MOTION COMPUTATIONAL IMAGING

Robert KAYEN<sup>1</sup>, Stefano GORI<sup>2</sup>, Bret LINGWALL<sup>3</sup>, Fabrizio GALADINI<sup>4</sup>, Emanuela FALCUCCI<sup>5</sup>,  
Kevin FRANKE<sup>6</sup>, Jonathan STEWART<sup>7</sup>, Paolo ZIMMARO<sup>8</sup>

### ABSTRACT

Between August and November 2016, three major earthquake events occurred in Central Italy. The first event, with M6.1, took place on 24 August 2016, the second (M5.9) on 26 October, and the third (M6.5) on 30 October 2016. As part of the Italy-US GEER team investigation, we recorded the amplitude and character of offset on the Mount Vettore Fault Zone (MVFZ) using traditional manual field recording and mapping techniques and advanced state-of-the-art geomatics methods of LIDAR and Structure From Motion.

Extensive field surveys by INGV geologists and the GEER team were performed on the flanks of Mt Vettore after the 24 August and 30 October events, and a limited survey was done between the two October events by INGV. These surveys indicated normal offset on several strands of the MVFZ, along the upper flanks of Mount Vettore and on the Piano Grande basin floor. The primary trace of the fault had measurable offset up to 215 cm in the northern section of the fault (42.810N-42.818N), and lesser offsets in the southern and central portion of the fault (42.796N-42.810N).

In tandem with the traditional field recording of offset, we collected TLS-LIDAR at several locations and flew approximately 5 km of the fault with unmanned aerial systems (UAS) to image the offsets. Lidar and Structure-from-Motion point cloud models were merged to construct a virtual topographic model of the fault. Comparison between the virtual offsets in the point cloud data and the field measurements at the same location found close agreement within 20% of the measured field values. The results indicate that LIDAR and UAS-based methods for collecting and analyzing topographic fault offsets are accurate and potentially greatly improve the magnitude of fault offset data sets from events with measurable surface rupture.

*Keywords: Fault Rupture; Earthquake; Geomatics, LIDAR, Structure-from-Motion*

### 1. INTRODUCTION

The 2016 central Italy earthquake sequence produced distinctive surface faulting on the Mt. Vettore-Mt. Bove normal fault system. Using a combination of Unmanned Aerial System (UAS)-based 3D Structure-From-Motion (SFM) models of topography and Terrestrial Laser Scans (TLS), we compared remotely sensed data with direct ground measurements to assess the ability of these technologies for evaluating surface rupture from two of the three mainshocks of the sequence: 24 August 2016 (M6.1), and 30 October 2016 (M6.5). No SFM or TLS data were collected for the 26 October 2016 (M5.9)

---

<sup>1</sup>Senior Scientist & Professor, USGS & UCLA, Los Angeles, CA, USA, [rkayen@usgs.gov](mailto:rkayen@usgs.gov)

<sup>2</sup>Research Scientist, INGV, Rome, Italy, [stefano.gori@ingv.it](mailto:stefano.gori@ingv.it)

<sup>3</sup>Assist. Prof., Dept. Civil & Environmental Eng., SDSMT, Rapid City, SD, USA, [Bret.Lingwall@sdsmt.edu](mailto:Bret.Lingwall@sdsmt.edu)

<sup>4</sup>Research Scientist, INGV, Rome, Italy, [fabrizio.galadini@ingv.it](mailto:fabrizio.galadini@ingv.it)

<sup>5</sup>Research Scientist, INGV, Rome, Italy, [emanuela.falcucci@ingv.it](mailto:emanuela.falcucci@ingv.it)

<sup>6</sup>Assist. Prof., Dept. Civil & Environmental Eng., Brigham Young Univ, Provo, UT, USA, [kevin.franke@byu.edu](mailto:kevin.franke@byu.edu)

<sup>7</sup>Professor, Dept. Civil & Environmental Eng., UCLA, Los Angeles, CA, USA, [jstewart@seas.ucla.edu](mailto:jstewart@seas.ucla.edu)

<sup>8</sup>Post Doct. Appnt., Dept. Civil & Environmental Eng., UCLA, Los Angeles, CA, USA, [pzimmer@ucla.edu](mailto:pzimmer@ucla.edu)

event. All three data sets (SFM, TLS, and direct measure) include locations, slip amplitude and direction.

### 1.1 2016 central Italy earthquake sequence

Between August and November 2016, three major earthquake events occurred in Central Italy. The first event, with  $M6.1$ , took place on 24 August 2016, the second ( $M5.9$ ) on 26 October, and the third ( $M6.5$ ) on 30 October 2016. This earthquake sequence occurred in a gap between two earlier damaging events, the 1997  $M6.1$  Umbria-Marche earthquake to the north-west and the 2009  $M6.1$  L'Aquila earthquake to the south-east (Figure 1). This gap had been previously recognized as a zone of elevated risk (GdL INGV sul terremoto di Amatrice, 2016). These events occurred along the spine of the Apennine Mountain range on normal faults and had rake angles ranging from  $-80^\circ$  to  $-100^\circ$ . Each of these events produced substantial damage to local towns and villages. The 24 August event caused massive damages to the following villages: Arquata del Tronto, Accumoli, Amatrice, and Pescara del Tronto. In total, there were 299 fatalities ([www.ilgiornale.it](http://www.ilgiornale.it)), generally from collapses of unreinforced masonry dwellings. The October events caused significant new damage in the villages of Visso, Ussita, and Norcia, although they did not produce fatalities, since the area had largely been evacuated.

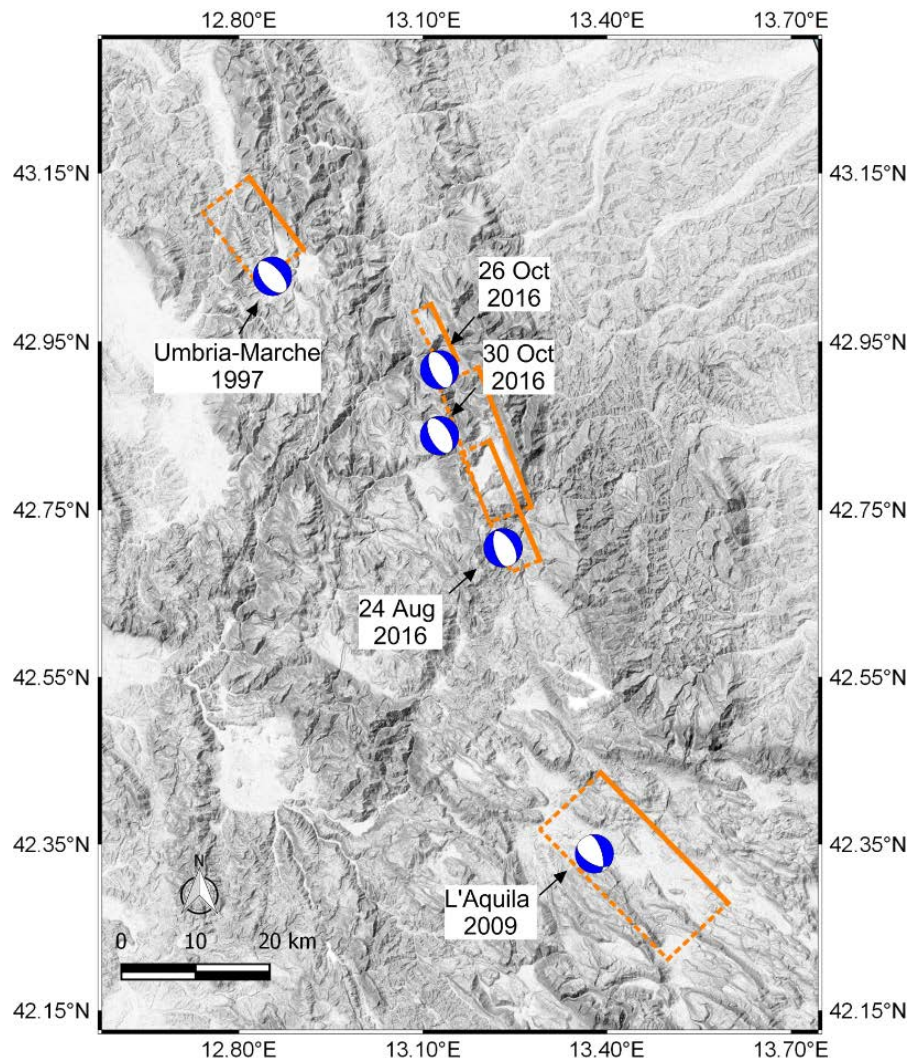


**Figure 1.** Map of central Italy showing moment tensors of major earthquakes since 1997 and the intermediate gap areas. Finite fault models from Chiaraluce et al. (2004; 1997 Umbria-Marche event), Piatanesi and Cirella (2009; 2009 L'Aquila event), Tinti et al. (2016, 24 August event), and GdL INGV sul terremoto in centro Italia, 2016, 26 and 30 October events). Moment tensors for 26 and 30 October 2016 earthquakes are also shown.

## ***1.2 GEER Reconnaissance***

The USNSF-funded Geotechnical Extreme Events Reconnaissance (GEER) association mobilized an Italian-USA team in two main phases following the 24 August event, and the two late October 2016 events. The reconnaissance objective was to collect and document perishable data that is essential to advance knowledge of earthquake effects. The Italy-US GEER team was multi-disciplinary, with expertise in geology, seismology, geomatics, geotechnical engineering, and structural engineering. Our approach was to combine traditional reconnaissance activities of on-ground recording and mapping of field conditions, with advanced imaging and damage detection routines enabled by state-of-the-art geomatics technology (GEER 2016; GEER 2017).

## **2. SURFACE FAULTING ON THE MT. VETTORE FAULT**

### ***2.1 Seismological Aspects of Mt. Vettore Fault***

The Mt. Vettore normal fault is NNW-SSE to NW-SE trending and can be detected for a length of about 18 km (Fig. 1, and is characterized by a fault scarp carved into the SW carbonate slopes of Sibillini Mts. The intermontane basin, the Castelluccio Plain, is associated with this fault. The basin is bordered by some of the fault splays located in the Piedmont area of Mt. Vettore. The most impressive fault scarp is represented by the “Cordone del Vettore” located at about 2,000 meters a.s.l. in the uppermost portion of the slope (Calamita and Pizzi, 1992; Coltorti and Farabollini, 1995; Cello et al., 1997; Pizzi et al., 2002; Pizzi and Galadini, 2009). Along the scarp, the exposed fault plane has displaced carbonate rocks that, in the hanging wall, are overlain by a thin and discontinuous cover of debris. Secondary fault activity is related to the displacement of the alluvial fan in the northern area of the Castelluccio basin. The displacement is due to the motion of a subsidiary fault section, parallel to the Cordone del Vettore (Galadini and Galli, 2003). The motion of these secondary faults, paleoseismologically investigated in 1999.

No historical earthquake is associated with this fault system. Paleoseismological data attribute the last fault activity to the beginning of the first millennium B.C. (Galadini and Galli, 2003; Galli et al., 2008). This fault system was one of two fault segments involved in the 24 August event (GEER, 2016). The 30 October event re-ruptured the southern 4.8 km of the fault and extended that rupture to the north, producing an overall rupture length of approximately 15-20 km. Figure 2 shows the length of the surface rupture as recorded by GdL INGV sul terremoto in center Italia (2016) and observations by INGV members of the GEER team.

### ***2.2 Physical direct measurement of the fault rupture***

We performed detailed direct measurement of fault rupture on the main scarp along the southern and southwestern flanks of Mt. Vettore, and on the secondary fault offsets observed in Castelluccio plain. The 24 August event produced displacements on the main fault trace ranging from null to 35 cm (mostly 10-25 cm). Details of the direct physical measurement of surface rupture for the 24 August event is described in GEER (2016), although there is no corresponding remotely sensed data. The level of documentation of surface rupture effects is mixed for the October events classified as main shocks (26 and 30 October). For the 26 October 2016 event, minimal direct field observations were documented in the short time window between this event and the subsequent 30 October event. Rapid and limited field surveys by INGV geologists after the 26 October event revealed surface rupture features with amounts ranging from 5 to 18 cm. These minimal observations established the presence of fresh surface rupture with additional slip.

The 30 October event saw several phases of detailed reconnaissance in late November and early December that established new fault segments on which rupture was observed, and a detailed picture on the amounts and distribution of slip in many areas that had previously faulted. The full length of the fault rupture was not mapped due to the onset of winter that closes roads in this alpine region.



Following the October 30 event, we found in some of the areas displaced in August had cumulative slip of upwards of ~210 cm on the main fault trace(42.81687°N, 13.25503°E). Displacements of up to several tens of cm (generally below 10 cm) were also observed on the secondary fault crossing the Castelluccio Plain (Figure 3), that had not displaced on the 24 August event.

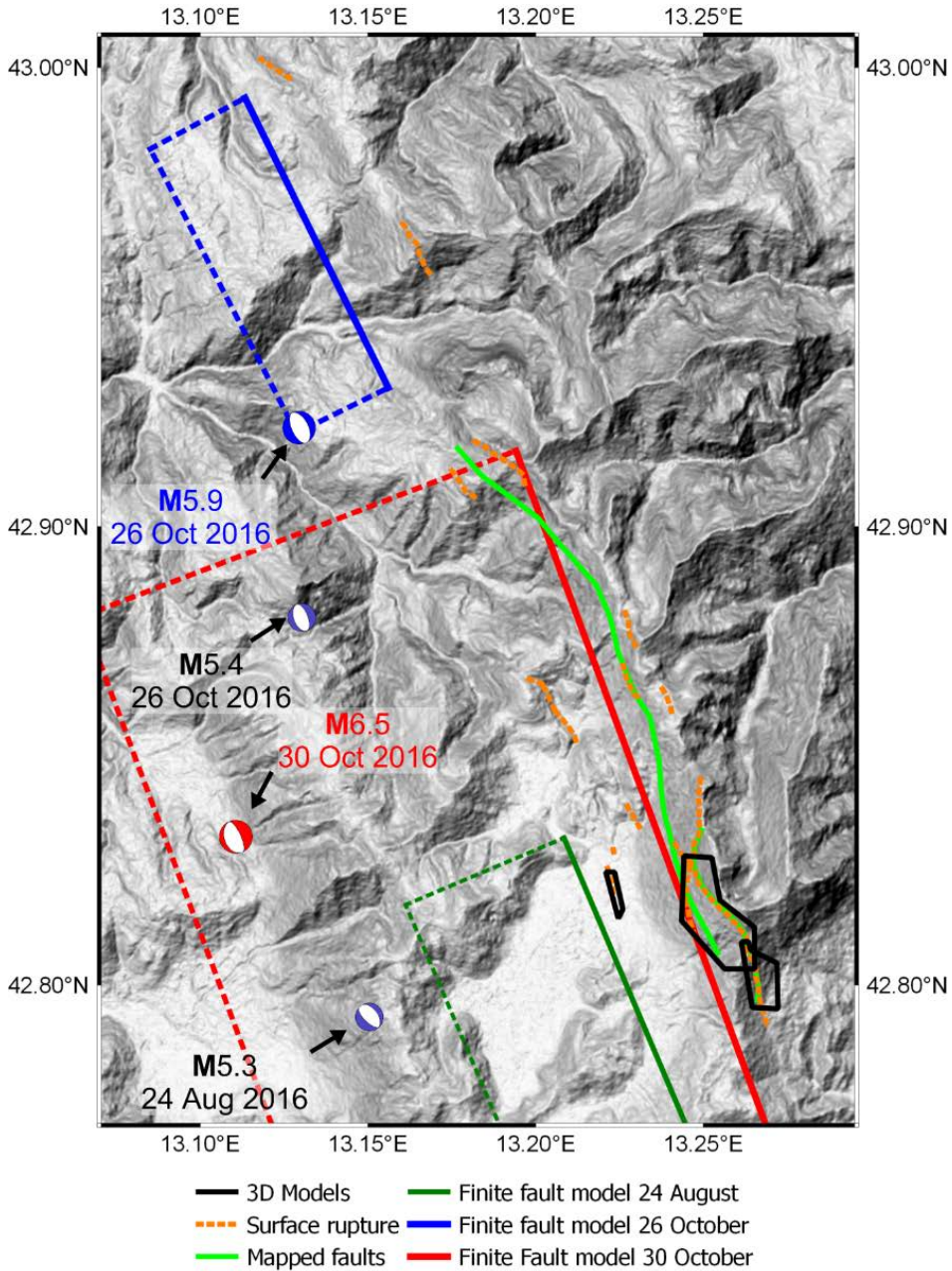


**Figure 2.** Detailed map of surface fault rupture, pre-event mapping of Mt. Vettore-Mt. Bove (blue) and Norcia (green) fault systems, and locations of 3D models.

**3. SFM AND LIDAR DATA FOLLOWING 26 OCTOBER 2016 EVENT**

Reconnaissance of surface fault rupture following the 30 October event consisted of three principle elements: [1] Observations of fault segments with and without new surface rupture; [2] two phases of detailed mapping of surface rupture locations and direct measurement of displacements using rulers and tape measures by GEER; and [3] imaging of the deformed ground surface at and near the fault

through the use of unmanned aerial systems (UAS) and terrestrial laser scanning, also by GEER. Figure 2 shows the broad area in which these observations of rupture were measured.

An important point to make here is that surface rupture observations at any point in time represent the cumulative slip from all prior events. Hence, the only way to evaluate slip from any particular event is through the differencing of multi-epoch displacement measurements. Detailed, by hand, mapping was conducted following the 24 August event (GEER 2016) for the southern portion of the Mt Vettore fault. Because such areas did not experience slip in the 26 October event, but were observed to have additional displacements in our December 2016 reconnaissance, such differentials can be attributed to the 30 October event. As an example, Figure 3 shows a location near the south end of the fault rupture close to road SP477 where multi-epoch photographs and measurements are available, showing the much larger slip in these areas from the second, 30 October, event.

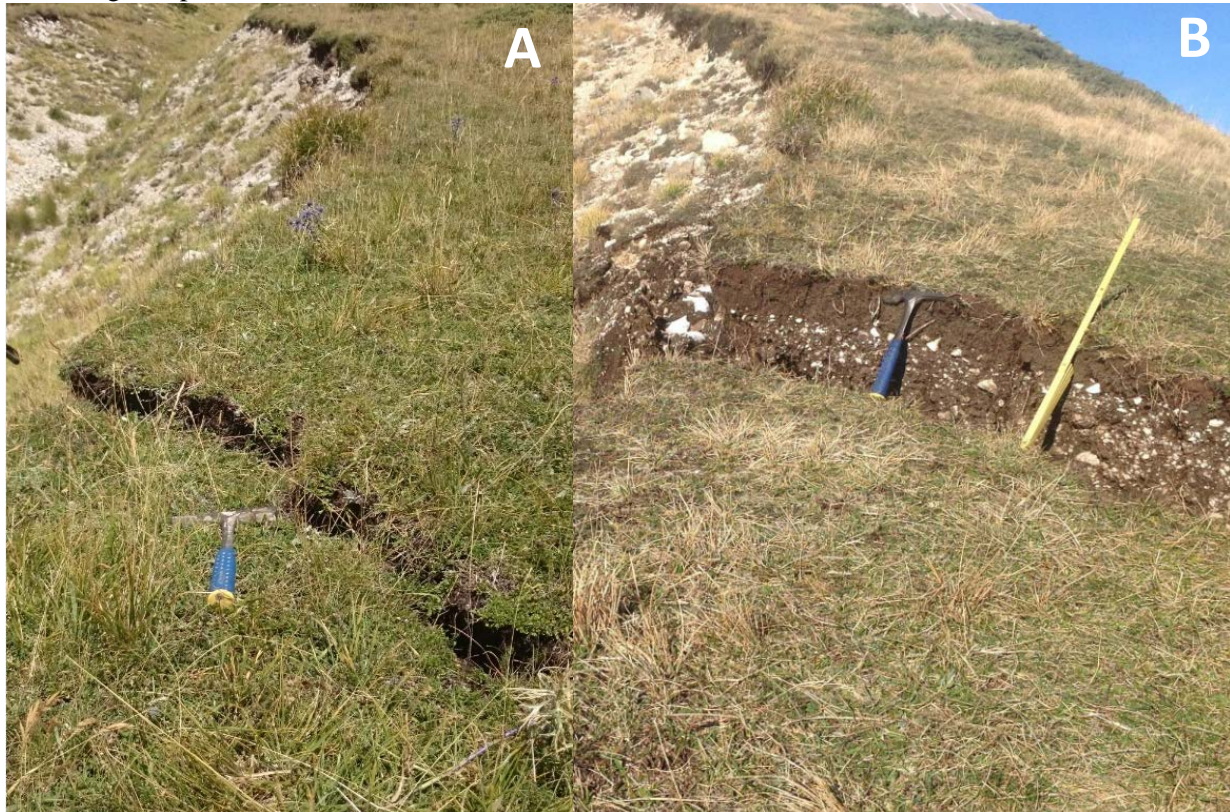


**Figure 3.** Comparative fault offset: (a) Vertical offset of 10cm from the August event, and (b) 30cm Vertical offset from the October 2016 events on the south face of Mt. Vettore near road SP477. Horizontal offsets were 0cm and 2cm. Lat = 42.79795, Long = 13.26607.

### ***3.1 SFM and TLS methodology***

Computational imaging methods using unmanned-aerial-systems (UAS), Structure-from Motion (SFM) matrix methods, and LIDAR-based terrestrial laser scanning (TLS) were used to conduct mapping, and to compare remotely sensed imagery with direct physical measurements using rod and tape. The GEER geomatics team collected new SFM photogrammetric data with DJI Phantom 4 drone equipped with a 20 megapixel lens. These data were collected at low elevations of less than 50 m, and high elevations greater than 100m over the fault. Flying the UAS over steeply sloping ground was challenging.





**Figure 4.** UAS/TLS-based orthomosaic model of the SW face of the Mt. Vettore Massif after the 30 October earthquake with 3D digital terrain model from merged SfM and LiDAR data. Approximate main fault trace(s) indicated in yellow, a second 1 km long visible trace of the “Western Trace” shown in white. Looking from the west. The left of the image is to the north. The slope moves from top to bottom of the image.

Point cloud data from the UAS are processed through a computationally intensive multi-stage process. First, a flight plan is established to overfly the fault and collect downward looking photographs using a Phantom 4 UAS quad-copter. These images were collected with a minimum of 80% overlap and 80% side-lap coverage to ensure that there are common features in adjacent images. Using cloud computing software from 'Dronedeploy,' and workstation-based software 'ContextCapture' from Bentley Software and 'Photoscan' from Agisoft, all of the downward-looking images were aligned using hard features that were common to multiple photographs. Images were first aligned crudely, and then a sequence of higher level alignments improved the model and established a tight relationship between adjacent images. The structure-from-motion method computes angular separations between objects visible in overlapping images. The scale and location of the objects are determined by knowing the location of each photograph from the photo metadata GPS-location. That is, the GPS-tagged photographs from the drone provided the scale for the model.

Aligned drone imagery was used to process a dense point cloud and a 3-D mesh triangular irregular network surface. The same aligned imagery was used to construct a precise orthomosaic of the scanned area. Once the UAS model was constructed, the point cloud from the UAS data can be merged with the point cloud from the Lidar scanner. UAS and LiDAR datasets are merged using the software ISITE-Studio (Maptek company). The advantage of merging data is that the Lidar data-set is presumably more precise regarding pixel location, whereas the UAS data have a more accurate color representation for each pixel because of the direct relationship between the point cloud and the orthomosaic image.

Terrestrial laser scan data was collected on sections of the fault rupture. The GEER TLS system is based on a near-infrared laser transceiver manufactured by Riegl (<http://www.rieglusa.com/>). The system is portable and designed for the rapid acquisition of high-resolution three-dimensional imagery under outdoor conditions. The maximum distance to targets the laser can detect is 1000m for an object with 80% reflectance under the best atmospheric conditions. The minimum target distance is 2 m. The range accuracy is consistently 0.4cm. TLS systems also have the ability to collect real color object data. Lidar data was collected using the terrestrial laser scanning method. The scanner was placed on a tripod, and its GPS location was recorded. A point cloud of coordinates visible to the scanner is collected and registered with the other scans in the same area where overlapping data exists.

#### 4. COMPARISON OF THE SFM/TLS DATA WITH DIRECT HAND MEASUREMENTS

The data of vertical slip on the Mt. Vettore fault includes total cumulative slip, with the total displacement measured in the December reconnaissance. Additionally, the data include the September-to-December survey differential, which is calculated as the total cumulative slip from all three events (December reconnaissance measurements) minus the combined effects of 26 October and the 30 October event (remaining amount attributed to the August 24 event). These totals and differentials were measured along the southern portion of the Mt. Vettore fault rupture along the (Figure 5). An example of the multi-epoch fault displacements can be seen in Figure 6 (42.81724°N, 13.25449°E). The upper white band represents the slip from the August 24 event with an average displacement of 16 cm. The total offset for the three events is approximately 130 cm, leaving 114 attributable to the October events and any accumulated co-seismic slip.

We compare displacements along the primary (highest elevation) segment of the Mt. Vettore fault as measured by hand and from the 3D terrain model. These displacements were made along the portions of Mt. Vettore that are on the west face of the ridge and on the branch descending the ridge towards SP477. Since the December remotely sensed data represent the total cumulative offset on the fault, we compare the UAS/LIDAR data to the values of the open circles in Figure 5. Figure 7 shows comparative values of cumulative displacements across all events, which for this portion of the fault arise from the 24 August, 26 October, and 30 October 2016 events. The 3D model in these areas is based on merged UAV point cloud data and LIDAR data, and the displacements were measured from the model using the programs I-Site Studio and Dronedeploy. The comparison shows that the step observed in the remotely sensed data is similar in value to the hand measured value. It can be seen that the remotely sensed measures all fall within +/- 20% of the unity line. The comparison is considered quite good, with no clear evidence of bias. The clear expression of the normal slip on the fault and the lack of vegetation in the fault zone is likely the cause of the good comparative numbers.

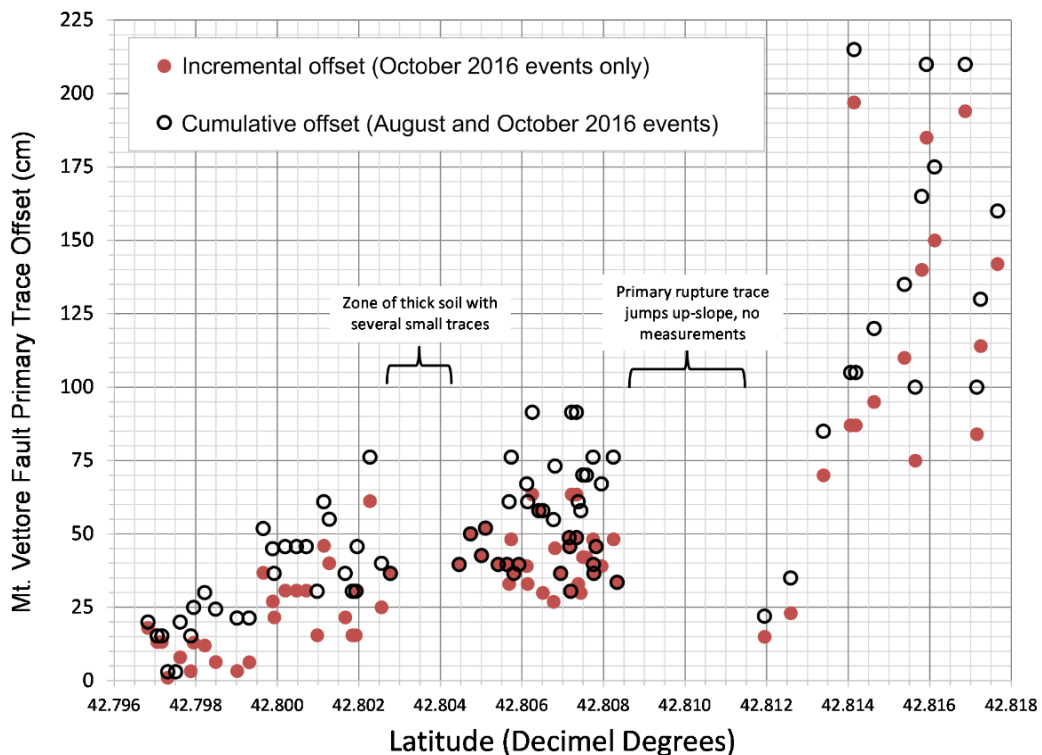


**Figure 5.** Distribution of differential and cumulative fault offsets for the southern half of the Mt. Vettore fault. All data in this Figure from hand measurements.





**Figure 6.** Example of fault slip measurements showing multi-epoch offsets from August 2016 (upper white band, 16 cm) and October 2016 (130 cm) events. Lat = 42.81724, Long = 13.25449.

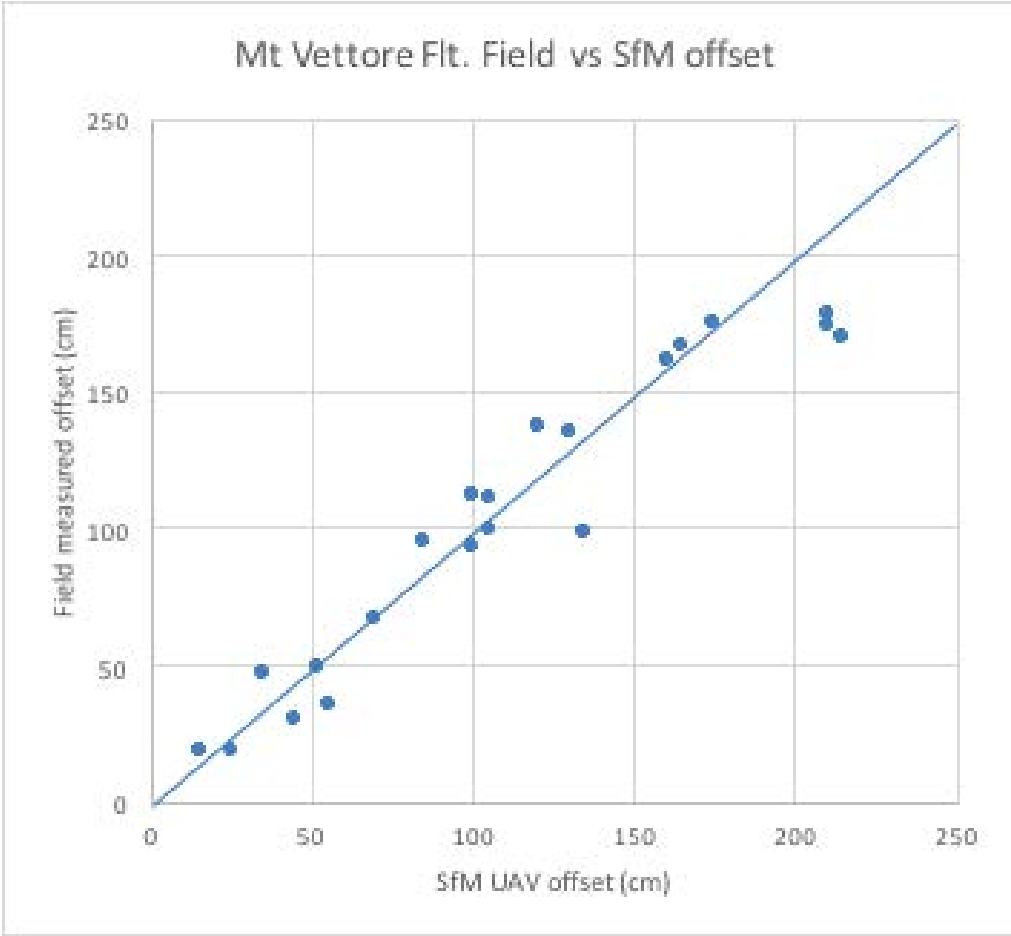


**Figure 7.** Surface fault rupture displacements from August-October event sequence as evaluated from hand measurements in the field and UAV-based 3D model.

## 5. CONCLUSIONS

Field surveys by the GEER team including INGV geologists were performed on the flanks of Mt Vettore after the 24 August and 30 October events. These surveys indicated normal offset on several strands of the MVFZ, along the upper flanks of Mount Vettore and on the Piano Grande basin floor. The primary trace of the fault had measurable offset up to 215 cm in the northern section of the fault (42.810N-42.818N), and lesser offsets in the southern and central portion of the fault (42.796N-42.810N).

We extended the range of field recording of the offset by augmenting the traditional hand measurements with data derived from TLS-LIDAR at several locations and data from structure-from-motion models gathered when we flew approximately 5 km of the fault with unmanned aerial systems (UAS) to image the offsets. Lidar and Structure-from-Motion point cloud models were merged to construct a virtual topographic model of the fault. Comparison between the virtual offsets in the point cloud data and the field measurements at the same location found close agreement within 20% of the measured field values. The results indicate that LIDAR and UAS-based methods for collecting and analyzing topographic fault offsets are accurate and can potentially greatly increase the magnitude of fault offset data sets from events with measurable surface rupture.

## 6. ACKNOWLEDGMENTS

The work of the GEER Association, in general, is based upon work supported in part by the National Foundation through the Geotechnical Engineering Program under Grant No. CMMI-1266418. The GEER Association is made possible by the vision and support of the NSF Geotechnical Engineering Program Directors: Dr. Richard Fragaszy and the late Dr. Cliff Astill.

## 7. REFERENCES

1. Galadini F. and Galli P., 2003. Paleoseismology of silent faults in the Central Apennines (Italy): the Mt. Vettore and Laga Mts. faults. *Annals of Geophysics*, 46, 815-836.
2. EMERGEO, 2016. Coseismic effects of the 2016 Amatrice seismic sequence: first geological results. *Annals of Geophysics*, **59**, Fast Track 5, 2016. DOI: 10.4401/ag-7195.
3. GEER, 2016. Engineering reconnaissance of the 24 August 2016 Central Italy Earthquake. Version 2, Zimmaro, P. and Stewart, J. P. (editors), Geotechnical Extreme Events Reconnaissance Association Report No. GEER- 050B. doi: 10.18118/G61S3Z.
4. GEER, 2017. Engineering reconnaissance following the October 2016 Central Italy Earthquakes - Version 2, Zimmaro, P. and Stewart, J. P. (editors), Geotechnical Extreme Events Reconnaissance Association Report No. GEER-050D. doi: 10.18118/G6HS39.
5. Falcucci E., S. Gori, F. Galadini, G. Fubelli, M. Moro, and M. Saroli, 2016. Active faults in the epi-central and mesoseismal MI 6.0 24, 2016 Amatrice earthquake region, central Italy. Methodological and seismotectonic issues. *Annals of geophysics*, **59**, Fast Track 5, 2016.
6. Gori et al., 2018, Surface Faulting Caused by the 2016 Central Italy Seismic Sequence. *Eleventh Nat. Conf Earthquake Engineering, June 25-29,2018, EERI, Los Angeles, CA*.
7. Commissione Tecnica per la Microzonazione Sismica, 2015. Linee guida per la gestione del territorio in aree interessate da Faglie Attive e Capaci (FAC), versione 1.0. Conferenza delle Regioni e delle Province Autonome– Dipartimento della Protezione Civile, Roma.